ROYAL SOCIETY OF CHEMISTRY

Spatially resolved flux measurements of NO$_x$ from London suggest significantly higher emissions than predicted by inventories

Adam R. Vaughan,[a] James D. Lee,*[b] Pawel K. Misztal,[c] Stefan Metzger,[de] Marvin D. Shaw,[b] Alastair C. Lewis,[b] Ruth M. Purvis,[b] David C. Carslaw,[bf] Allen H. Goldstein,[c] C. Nicholas Hewitt,[g] Brian Davison,[g] Sean D. Beevers[h] and Thomas G. Karl[i]

To date, direct validation of city-wide emissions inventories for air pollutants has been difficult or impossible. However, recent technological innovations now allow direct measurement of pollutant fluxes from cities, for comparison with emissions inventories, which are themselves commonly used for prediction of current and future air quality and to help guide abatement strategies. Fluxes of NO$_x$ were measured using the eddy-covariance technique from an aircraft flying at low altitude over London. The highest fluxes were observed over central London, with lower fluxes measured in suburban areas. A footprint model was used to estimate the spatial area from which the measured emissions occurred. This allowed comparison of the flux measurements to the UK's National Atmospheric Emissions Inventory (NAEI) for NO$_x$, with scaling factors used to account for the actual time of day, day of week and month of year of the measurement. The comparison suggests significant underestimation of NO$_x$ emissions in London by the NAEI, mainly due to its under-representation of real world road traffic emissions. A comparison was also carried out with an enhanced version of the inventory using real world driving emission factors and road measurement data taken from the London Atmospheric Emissions Inventory (LAEI). The measurement to inventory agreement was substantially improved using the enhanced version, showing the importance of fully accounting for road traffic, which is the dominant NO$_x$ emission source in London. In

[a]*Department of Chemistry, University of York, York, UK*

[b]*National Centre for Atmospheric Science, University of York, York, UK. E-mail: james.lee@york.ac.uk*

[c]*University of California, Berkeley, USA*

[d]*National Ecological Observatory Network, Boulder, USA*

[e]*University of Colorado, Boulder, USA*

[f]*Ricardo Energy and Environment, Fermi Avenue, Harwell, Oxon, OX11 0QR, UK*

[g]*Lancaster Environment Centre, Lancaster University, Lancaster, UK*

[h]*Department of Analytical and Environmental Sciences, King's College London, UK*

[i]*Institute of Atmospheric and Cryospheric Sciences, University of Innsbruck, Innsbruck, Austria*

central London there was still an underestimation by the inventory of 30–40% compared with flux measurements, suggesting significant improvements are still required in the NO_x emissions inventory.

Introduction

Due to its adverse effects on human health,[1–4] nitrogen dioxide (NO_2) concentrations are regulated by the EU Air Quality Directive which sets limit values for hourly and annual mean ambient concentrations. The annual mean limit value of 40 μg m^{-3} is exceeded in many urban centres throughout the UK, including London. In addition to its direct health effects, NO_x (the sum of $NO + NO_2$) contributes to the formation of ozone and secondary particles through a series of photochemical reactions[5] and hence reductions in NO_x emissions are necessary to control the regional-scale ground level concentrations of ozone, which is itself a regulated pollutant under the Air Quality Directive.

Concentrations of carbon monoxide (CO) and hydrocarbons in urban centres in the UK have decreased by around an order of magnitude over the past 20 years, providing clear evidence of the effectiveness of both the legislative framework and the emission control technologies employed for these pollutants. However, whilst trends in ambient concentrations of NO_x and NO_2 in the UK generally showed a decrease in concentration from 1996 to 2002, this has been followed by a period of more stable concentrations from 2004 to 2014. This is not in line with the expected decrease suggested by the UK emission inventories (Fig. 1).[6]

It is known that ambient NO_2 does not respond linearly to reductions in the concentration of NO_x, in part due to changes in diesel emission control technology leading to increases in directly emitted NO_2,[7] and partly due to the complexities of atmospheric chemistry. This may partially explain why ambient concentrations of NO_x have not declined as rapidly as expected. Although it has been known for some time that on-road emissions of NO_x from diesel passenger cars are often higher than those measured during test cycles,[8] it has very recently emerged that this may be due to deliberate action by some manufacturers. The issues surrounding NO_x emission from diesel vehicles are exacerbated in Europe by the high proportion of diesel engine vehicles in the passenger car fleet.[9] Hence, not surprisingly, there remain considerable difficulties in reconciling predictions of changes in NO_x concentrations arrived at using emission inventories with actual measurements of ambient concentrations.

Air pollutant emission inventories provide input data for air pollution models, which in turn are used for predicting current and future air pollution and in developing strategies for improving air quality. One approach uses the so called 'bottom up' approach involving estimating emissions from different individual sources (*e.g.* emissions from a particular type of vehicle per km driven) and activity factors (*e.g.* number of vehicle km driven on a particular road) to produce annual emission estimates.[10] Therefore errors in the emissions from a large source sector (such as passenger cars) can lead to significant inaccuracies in the inventories, which then further propagate into forecasts of air pollutant levels. Evaluation of emission inventories can be carried out by comparing air quality model predictions (using inputs from the inventory) to observed concentrations. However this method does not provide a direct comparison with the emission rate

as it requires knowledge of other parameters such as chemistry and meteorology, as well as the inherent uncertainty in the models themselves. In contrast, the eddy-covariance technique provides a direct measurement of an atmospheric pollutant flux from a particular 'footprint', providing a 'top down' approach for quantifying emissions.[11]

A recent study from a tall tower site in central London[12] directly compared the measured NO_x emission rate with estimates from UK emissions inventories.[10,13] The study found observed emissions of NO_x were on average 80% higher than standard inventory estimates for central London, suggesting the inventory was poorest at estimating NO_x where traffic is the dominant source. Agreement was found to be better when an inventory with more explicit treatment of traffic emissions was used, so showing the importance of correctly accounting for the traffic source in London. While this tower-based study well represents the vicinity of the measurement location, it cannot reveal spatial patterning across Greater London.

In the present work, we report measurements of NO_x fluxes taken from a low flying aircraft over London. Full details of the flight tracks, as well as measurement concentrations of NO_x and volatile organic carbons (VOCs) from the aircraft (including a comparison to various ground based measurements in London) can be found in Shaw *et al.* (2015).[14] Here, we will concentrate exclusively on the flux measurements. Spatially resolved data are compared to emissions inventories, providing a measure of how well the inventories reproduce measured emissions over a wide area of central and suburban London.

Experimental

Measurements

Research flights were conducted using the Natural Environment Research Council's Dornier 228 aircraft, based at the NERC Airborne Research and Survey Facility (ARSF) at Gloucester Airport. Each flight operated with a crew of two pilots, a mission scientist and up to three instrument scientists. Flight speed was maintained at 80 m s^{-1} over central London, with a flight altitude for flux measurements of $\sim$360 m, ensuring measurements could be directly related to
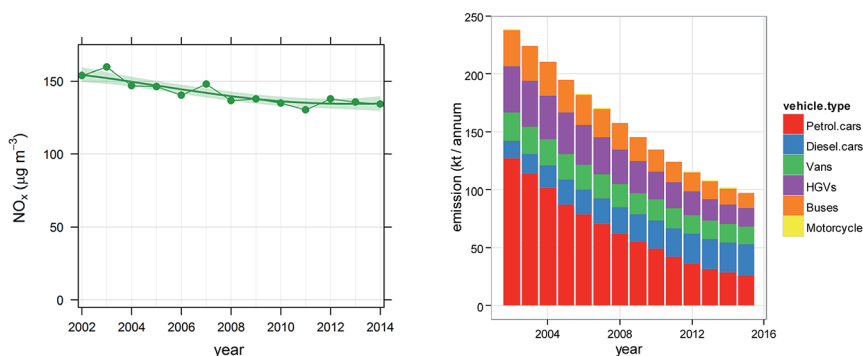

Fig. 1 (a) Trends in the mean concentration of NO_x across 35 roadside sites in Greater London with at least 10 years of data capture, (b) projected change in urban road transport emissions split by main vehicle type from the NAEI using 2002 as a base year.

the surface. The measurements ran over a two-week period during July 2013. In total 12 flights were completed across a set flight path, running from the south-western to north-eastern suburbs, of central London, crossing the River Thames in the vicinity of London Bridge and Tower Bridge. Each flight was designed to gain multiple replicate transects across the same flight path. The flight path was chosen to allow flux measurements to be made over a representative sample of land use types in London. Flight times were staggered over the two weeks to allow for study into the rush-hour periods, as well as weekday to weekend comparisons.

Measurement of NO_x (NO and NO_2) mixing ratios were made using a chemiluminescence instrument designed for 10 Hz measurements, via dual channel design to allow concurrent measurement of NO and NO_2.[15] The instrument quantifies NO via chemiluminescence upon its reaction with excess O_3, and NO_2 indirectly using a photolytic converter to convert NO_2 to NO at 395 nm, followed by detection by chemiluminescence.[16] A more detailed description of the running, calibration and design of the instrument can be found in Shaw et al. (2015).[14] Mixing ratios used in this study are reported with respect to dry air + water vapour, due to constant stable humidification of the O_3 reactant used in the instrument. An accurate humidity value within the sample volume was not obtained. Humidification of the reaction O_3 is conducted to remove any changes in background signal caused by rapid water vapour changes in the ambient sample during the flights. Due to this the reported wet mixing ratios are lower compared to dry mixing ratios, and a potential underestimation of the NO_x flux was calculated to not exceed 4%.

During all flights, an Aircraft-Integrated Meteorological Measurement System (AIMMS 20) turbulence probe (Aventech Research Inc.) mounted underwing was used to obtain micrometeorological measurements at a 20 Hz acquisition rate.[17] The probe was calibrated for static and dynamic upwash.

Wavelet transformation

In this study, we build upon previous work described by Torrence and Compo (1998) and Thomas and Foken (2007) and use the continuous wavelet transform (CWT) methodology for quantifying eddy-covariance fluxes from an aircraft.[18,19] We conduct CWT via eqn (1), defining the transform of the discrete data sequence $x(n)$ via complex conjugate of the Morlet wavelet $\psi^*_{p,a,b}$, for N data points[20]

$$w_x(a,b) = \sum_{n=0}^{N} x(n)\psi^*_{p,a,b}(n) \tag{1}$$

ψ denotes the mother wavelet, with a and b acting as parameters to scale and localise the wavelet in frequency and time respectively, and p as the normalized factor. In order to fully portray our approach, it is useful to understand the properties of a wavelet. The base equation for a wavelet is coined by the mother wavelet after localisation has occurred. This is defined in eqn (2).[21]

$$\psi_{a,b}(t) = \frac{1}{\sqrt{a}}\psi\left(\frac{t-b}{a}\right) \tag{2}$$

Wavelets are localised both in the frequency domain as for Fast Fourier Transform (FFT) but also in the time domain.[22] This allows for a signal's

properties to be explored in both domains. Another added strength of the method is the ability to tailor the wavelet's properties to suit the application. In this study we used the complex Morlet wavelet as expressed in eqn (3).[18]

$$\psi_0(\eta) = \pi^{-1/4}e^{i\omega_0\eta}e^{-\eta^2/2} \qquad (3)$$

ω_0 represents the frequency and η the time parameter in non-dimensional state. A more in-depth description for wavelet principles and the Morlet wavelet can be found in Torrence and Compo.[18] The Morlet wavelet has been implemented in a number of previous studies specifically for analysing airborne measurements.[20,21,23–25]

Flux calculations

Flux is the measure of the rate of change of a quantity moving through an area per unit time, in this case, the amount of a chemical species (NO and/or NO_2) being uplifted at a point in space per unit time. In order to quantify this, we implement a flux calculation algorithm developed and previously used in airborne studies of isoprene fluxes.[25] Using CWT, the covariance between vertical wind and species of interest is evaluated. We first calculate the lag time difference between vertical wind speed (w') and analyte concentration (c'), where w' represents the difference of the instantaneous vertical wind measurement to the mean vertical wind and c' is the difference of the instantaneous concentration (mixing ratio) to the mean concentration value. This allows the two data sets to be aligned, giving normalised covariance.

The lag time between the two data sets was found to be in the range of 4–7 s. Due to the observed non-stationarity of the lag difference, each flight leg was analysed separately ensuring no additional bias. Before we calculated fluxes *via* CWT, de-spiking of the data was conducted. The CWT calculates the global cross-spectrum between analyte concentration and vertical wind speed. Fig. 2(b) depicts an example of the global cross-spectrum for a flight leg of NO_2 concentration data, with the *y*-axis giving the eddy contributions integrated over all frequency periods in seconds and the *x*-axis being the distance travelled along the flight leg. For each individual flight leg, we compared the co- and cumulative spectra across all frequencies for both the CWT and a standard Fast Fourier Transform (FFT). For all the flight legs, the majority of the flux contributions were found to be below 0.1 Hz. This inferred that high frequency spectra correction was not needed, with its contribution to the calculated flux being low. As a final data quality tool, we pad the edges of the wavelet with zeros to help remove any associated edge effects. After this padding is done we apply the cone of influence (COI). The COI is defined as the area outside of which edge effects in the wavelet cross-spectrum give rise to data of a lower quality than the rest.[18] For this reason we only consider data within the COI, and remove all other data. Due to the reactive chemistry between NO and NO_2 in the presence of O_3,[26] we calculated NO_x flux *via* separate flux calculations for NO and NO_2, with the combination of the two yielding total NO_x flux.

Error analysis

Error quantification for the instantaneous fluxes was conducted as previously described by Karl *et al.* (2009), with the total error for the calculated flux being due to both random (re) and systematic (se) errors.[23]
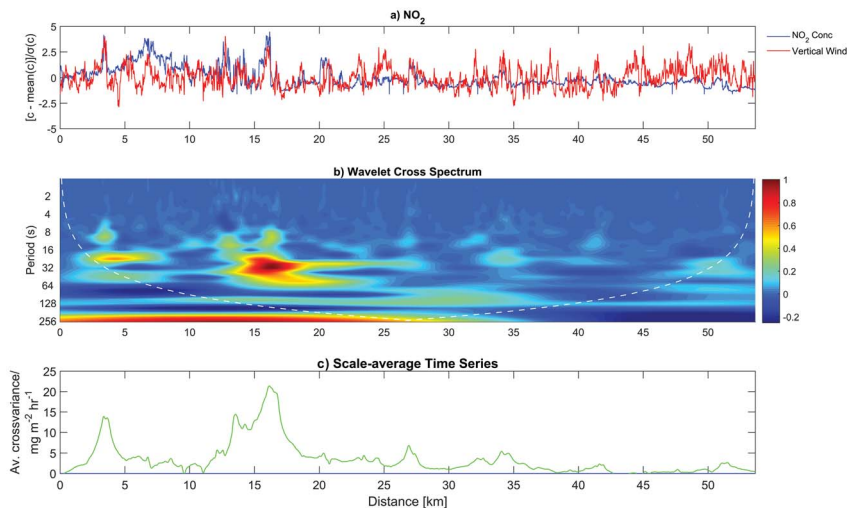
Fig. 2 (a) Variation of NO_2 mixing ratio from the mean and variance of vertical wind speed from the mean, (b) time resolved wavelet cross spectrum, (c) the average cross-covariance between NO_2 mixing ratio and vertical wind, for a typical NE to SW run across London.

$$re \leq 1.75 \left(\frac{z}{z_i}\right)^{0.25} \left(\frac{z_i}{L}\right)^{0.5} \tag{4}$$

$$se \leq \frac{2.2 z_i \left(\frac{z}{z_i}\right)^{0.50}}{L} \tag{5}$$

L denotes the flight leg length, z the flight altitude and z_i the height of the boundary layer. Boundary layer heights were obtained at the beginning and end of each flight *via* atmospheric soundings from Heathrow Airport, west of London. A more detailed study into the relative effects of errors for calculated flux measures can be found in Mann and Lenschow (1994).[27] We find calculated systematic sampling error for the entire flight leg to vary from 1–4%, with random sampling error being the major contributor to the overall error, varying from 15–25%. We also account for the 4% error associated with humidity, giving a total error for the flux estimates in the region of 20–35%. In order to provide meaningful comparison with emission inventories, the random sampling error was also calculated individually for each 1 km resolved flux measurement, and found to range from 60–250%. Errors associated with chemical and physical losses and storage of NO_x in the city canopy below flight level are discussed in detail below.

Footprint model

In order to carry out interpretation of the data and compare to emissions inventories, it is necessary to calculate a flux footprint for each measurement. For this we use a footprint model which quantifies the spatial area from which the emission originates from.[28–30] An in-depth review into footprint models and their continued development can be found in Leclerc and Foken (2014).[31] We use the

footprint model described by Metzger *et al.* (2012),[32] due to its similar application.[21] This builds upon a cross-wind integrated model, which quantifies the flux contribution relative to the distance away from the measurement position, into the prevailing wind direction. This approach alone still leaves uncertainty due to the analysis being only in 1-dimensional space.[33] For this purpose Metzger *et al.* (2012)[32] coupled the model with a cross-wind function, allowing for non-perpendicular wind direction influences to be accounted for.

We parametrise the model using friction velocity, measurement height, standard deviation of the vertical wind and roughness length. Turbulence statistics for the footprint model are calculated at 1 km intervals from the wavelet cross-scalogram, with movement in both the x and y direction being 1 km for each new footprint. We use the Drew *et al.* (2013) study data to estimate expected roughness lengths for the London area.[33] For suburban area roughness lengths, values generally range from 0.4–0.6 m but up to 2.0 m for central London. The model evaluates the maximum influence distances in all directions, with the measurement point at its centre. From this it is possible to create a weighing matrix at the same temporal resolution as the inventories being quantified. The matrix when summed up gives a value of 1. This weighting matrix predicts, for every overflown 1000 m cell, the ground influence contributing to the observed emission flux. The matrix is set to the same coordinate system as the inventory. A separate weighting matrix is calculated for every measurement point along the flight track to allow for independent comparison.

For each point along the flight track, the emission inventory value for every cell within the footprint matrix is weighted accordingly and summed up to give a single emission estimate. All estimates from all source sectors are summed to give a total emission estimate every 1 km. Fig. 3 depicts an example of the area for which we can consider our measurements to be spatially representative. The footprint area ranges in distance from the flight track anywhere from 5 to 12 km into the prevailing westerly wind direction. Part of the footprint area includes part of the London Low Emissions Zone (LEZ) which was introduced in 2008 to help improve air quality in central London.
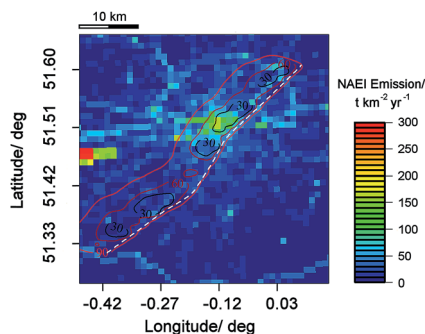

Fig. 3   The contributing footprint area to a typical flight track, dependent on the prevailing wind direction and altitude of flight. The footprint is overlaid onto the NAEI at 1 km² grid resolution, coloured to annual NO_x tonnage emission estimates.

Results

Flight descriptions

Due to problems with the AIMMS probe, here we only calculate NO_x fluxes from data collected on three flights (research flights 5, 7 and 12), from 3rd to 9th July 2013 (see Table 1). Each flight was planned to follow a set flight track over central London, containing multiple legs back and forth in north-easterly (NE) and south-westerly directions (SW), to allow for repeat measurements over the same area. Each flight started at the SW corner of the M25 ring road and proceeded across central London over the Tower Bridge area, to finally end at the NE corner of the M25. The leg was then reversed and repeated 7 or 8 times for each flight. Flight 5 was conducted during the morning rush hour from 08:00 until 10:00 am. Flights 7 and 12 were performed during the afternoon (12:00 to 16:00), thus providing some diurnal information of the emissions. Flights 5 and 7 had wind directions from the west, giving information about the emissions coming from central London. Flight 12 had wind directions prevailing from the NE giving emission information from more easterly areas of London. All the flights were performed during clear sunny days with the highest air temperatures observed (>23 °C) during flight 12. Further information of the flights including mixing ratios observed and comparisons to ground level observations can be found in Shaw *et al.* (2015).[14]

Spatially resolved flux observations

Calculated fluxes across all flights showed significant variability along the flight track. Fig. 4 shows all flight legs across London for flights 5, 7 and 12 (total of 17 legs). Each data point at 1 km resolution is coloured by measured NO_x flux. Consistently, the highest observed fluxes all coincide within the same spatial area, in central London. This area of London contains high traffic densities, a high density of large buildings and also the London Bridge railway station with a large number of diesel trains operating in the area. Measured NO_x fluxes over this area ranged from 30–90 mg m^{-2} h^{-1}, with the highest fluxes observed during flight 5. This corresponded to the morning rush hour period from 08:00 to 10:00 with high traffic densities in central London.[34] Fluxes measured on the other flights over central London during the afternoon showed consistently lower NO_x fluxes compared to the morning flights, in the range of 30–40 mg m^{-2} h^{-1}, with no clearly defined evening rush hour period obvious. For all flights, fluxes measured outside of central London (both in the SW and NE directions) were significantly lower, typically in the range 5–10 mg m^{-2} h^{-1}, corresponding to the lower traffic density in these parts of the city. Some spikes in NO_x fluxes, up to 20 mg m^{-2} h^{-1},

Table 1 Details of the flights where NO_x fluxes were calculated

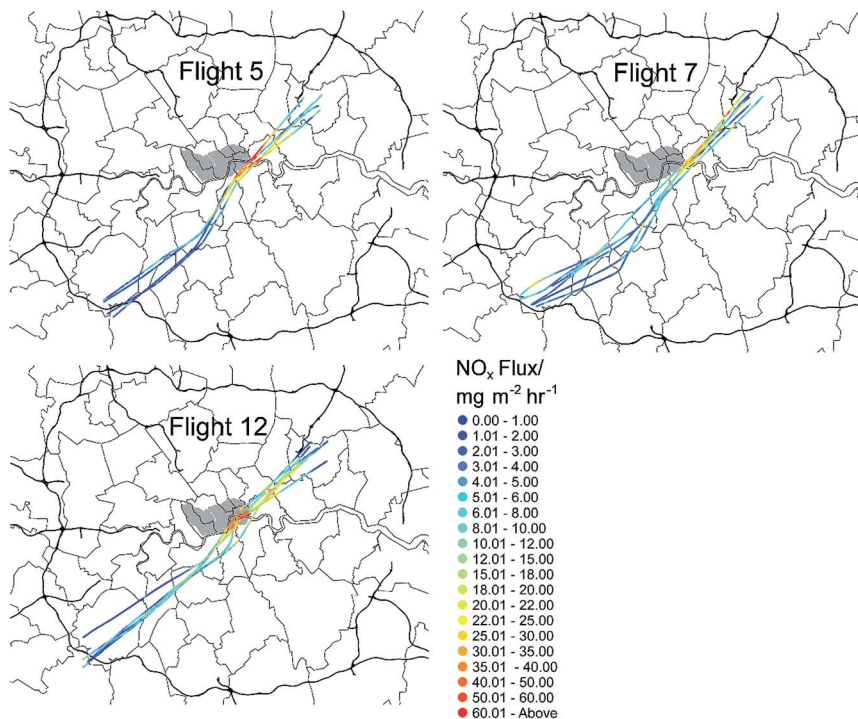| Flight number	Number of flight legs	Day of week	Time of day	Flight altitude/m	Wind direction/deg	Air temperature/°C
5	9	Wed	Morning	365–380	250–280°	14.0–16.0
7	7	Thurs	Afternoon	340–380	220–260°	19.0–21.0
12	7	Tues	Afternoon	340–360	30–70°	22.0–23.5

NOₓ Flux/
mg m⁻² hr⁻¹

Fig. 4 Tracks of all the flight legs for flights 5 (3rd July 2013 morning), 7 (4th July 2013 afternoon) and 12 (9th July 2013 afternoon), mapped over Greater London, coloured to the measured NOₓ flux. The grey area represents London's Low Emission's Zone (LEZ).

were observed on some legs, which seem to correspond with major roads (*e.g.* the M25 ring road).

Emission inventories

The UK's National Atmospheric Emissions Inventory (NAEI) is the standard tool for both reporting and understanding the emissions of a range of pollutants in the UK. For each pollutant the inventory is broken down into a series of source types which, when grouped and summed together, give an annual emission estimate at 1 km² resolution across the entire country. Emission source types include road transport, rail and aviation, domestic and industrial combustion, energy generation and other sources such as waste production.[35] In common with many other emission inventories in Europe, the NAEI is mainly based on the (Calculation of Emissions from Road Transport) COPERT 4 emission factor model for road vehicle emissions. The COPERT 4 methodology is part of the European Monitoring and Evaluation Programme/European Economic Area (EMEP/EEA) air pollutant emission inventory guidebook for the calculation of air pollutant emissions.[36]

To allow for real time comparison between our airborne flux measurements and the inventory estimates for the relevant flux footprint, each inventory source sector is assessed individually using the described footprint method in Section

2.5, giving an emission contribution. The emission inventories used here only provide annual emission estimates for each grid square from the wide range of source sectors – they do not directly provide temporally-resolved hour of the day or day of the year estimates. Therefore, we scale each source sector separately, using scaling factors[35] that take into account the temporal variation in emissions for any given month, day and hour. By scaling each source sector individually, we generate more realistic emission estimates for the specific time of day and day of the year of our flux measurements. Scaled estimates for each source sector are then summed up at each point along the flight track, to give 1 km resolution estimates for NO_x emission. Nevertheless, such temporal profiles represent the typical average profiles expected for different emission sources. Uncertainty will be introduced when comparing estimates obtained over short periods of time with the mean profiles used in atmospheric emission inventories.

Fig. 5 depicts the 1 km spatially resolved NO_x flux observations averaged for all three flights in blue and the NAEI emission estimates plotted in red for all flight legs, all against latitude of the sample position along the flight track. For all of the flights there is relatively good agreement between the NAEI estimates and the measurements in suburban outer London, but, there appears to be a significant underestimation in the inventory compared with the measurements, by a factor of 2–4, in central London (latitude 51.43–51.52). The data interpretation is complicated by the significant uncertainty (60–250%) in our 1 km spatially-resolved flux measurements. Therefore in order to further reduce these uncertainties, each flight track is divided into four parts, each approximately 11 km in length. The first two segments represent outer regions of SW London (zones 1 and 2) and the second set (zones 3 and 4) for central and NE London. The flux data are then averaged for each segment to give a single NO_x emission flux. The uncertainty associated for these fluxes is greatly reduced compared to the more spatially resolved flux data, as shown in Fig. 5, now being in the range 30–45%.

Fig. 6 depicts the average ratios of the measured to emission inventory-estimated fluxes from all the flight legs. The error bars denote the standard error of the 17 legs. Zones 1 and 2 in outer London show ratios of around 1.5, with the ratio increasing to over 2 for zones 3 and 4. These discrepancies are similar in magnitude to those reported from measurements made by Lee et al. (2015)[12] from 180 m above ground level on the BT Tower in central London.
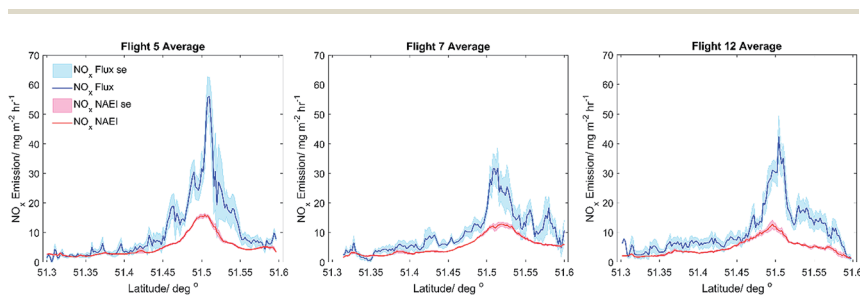

Fig. 5   Average for Flights 5, 7 and 12, measured NO_x flux plotted in blue with standard error as the shaded blue area. Calculated and scaled NAEI estimates of NO_x emission are plotted in red, with standard error as the shaded red area.
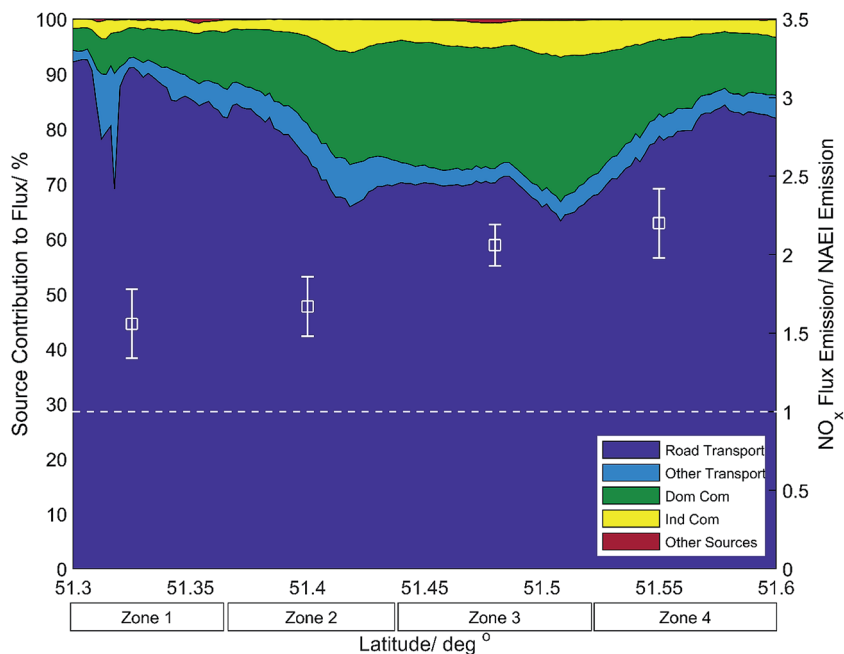
Fig. 6 Calculated emission source contributions from the NAEI plotted on the first y axis, with sources being broken down into road transport; other transport (such as rail), domestic and commercial combustion, industrial combustion and other sources. Also plotted on the second y axis as white squares is the ratio of measured to NAEI estimated NO_x flux, with the error bars denoting the standard error of all points included. The flight is broken into 4 zones, with 1 and 2 being SW outer London, 3 central London and 4 NE outer London.

It is clear that the NAEI is unable to accurately represent emissions of NO_x from London, with particularly large discrepancies in the central London area. One possible explanation for this is in the way in which the inventory accounts for road transport emissions. Fig. 6 shows that across the whole of the area surveyed by our flights, road transport is the dominant source of NO_x. Traffic contributes up to 90% of NO_x emissions in outer London (zones 1 and 2), strongly suggesting that significant error in the road traffic source in the inventory is responsible for the underestimation of NO_x emissions by the inventory relative to our flux observations. In central and NE London (zones 3 and 4), where the underestimation of the inventory is highest, road transport, while still the largest source, is responsible for 65–70% of the total NO_x emissions in the inventory, with most of the remainder due to domestic and commercial combustion of gas for space and water heating. The relatively low use of gas for heating during July is taken account of *via* the emission scaling factors applied to the NAEI, but the large underestimation in the inventory in the central London area suggests that as well as underestimation of traffic-derived NO_x, there is also some error in the NAEI treatment of domestic and commercial combustion, or there is a major missing source of NO_x in the inventory.

The results described above are potentially important as the NAEI is used to provide emissions for air quality forecasting models, which inform potential

future air quality abatement strategies. The following sections will discuss potential reasons for the discrepancy, including measurement errors and investigate the advantages of using a more London-specific emissions inventory with a more explicit treatment of the road traffic source.

Discussion

Measurement errors

Using the method of Karl et al. (2013)[24] we are able to quantify a limit of detection (LOD) for our flux measurements from the calculated covariance function, above which the measured flux can be distinguished from the combined effects of instrument noise.[24,37] We find the LOD varies from flight to flight, being in the range 0.075–0.180 mg m^{-2} h^{-1}, with our measured data almost always significantly above this.

Some NO$_x$ emitted at the ground surface may be lost before it is detected at the flight altitude, causing an error in our flux estimates. Using measured meteorological parameters and the wavelet transform, we calculate Deardorff velocities (w^*) for each flight. w^* gives a turn-over time for all the influencing eddies which account for the measured flux. We found w^* to be in the range of 0.5–3.0 m s^{-1}, which gives a vertical ascent time of 2–8 minutes from the surface to the measurement altitude of 300 m.

Loss of emitted substances can occur via three mechanisms: chemical reaction, weakening vertical transport and storage. To account for chemical losses in the atmosphere, we use the vertical flux profiles obtained in the Karl et al. (2013) study.[24] They were able to calculate the loss of isoprene emission during transport through the boundary layer. To use this method for NO$_x$, we substitute NO$_x$ chemistry into the model in place of isoprene chemistry, so taking into account the lifetime of NO$_x$ in the troposphere with respect to chemical reaction of NO$_x$ with the hydroxyl radical (OH). We use the middle-of-the-day OH abundances measured in London during summer 2012, as reported in the Lee et al. (2015) study,[38] of 2.0×10^6 molecule per cm^3. This gives a lifetime of NO$_x$ above London of ~11 hours. Using this calculated NO$_x$ lifetime, we estimate that the loss of NO$_x$ flux between the ground surface and the flight altitude is only between 1 and 2%. We have not considered other chemical NO$_x$ loss processes (e.g. PAN formation) as we believe these will be small compared to the reaction of NO$_2$ with OH. Loss due to weakening vertical transport accounts for the loss due to vertical momentum decreasing as altitude increases and is estimated to be 25–30%. The final loss process involves storage of some of the emission within the urban structure, such as street canyons.[39,40] However we do not consider this to be an important loss process here. Significant storage of NO$_x$ within the street canyon in London would result in a steady build up of concentrations, something that is not typically observed. Thus, if deposition processes are ignored, the transfer of NO$_x$ out of the street canyon is essentially equal to the emissions, with the only result being a potential time lag from emission to measurement. Future work in this area could gain from using the Lenschow et al. (2015) study to account for all three loss terms in unison.[41] All of these loss processes have the potential to increase our measured fluxes, which would further increase the discrepancy between measured and inventory-estimated emissions.

As discussed above, our study shows that, even in outer London where traffic sources are estimated to contribute 90% of the emitted NO_x, there is observed inventory under-estimation by a factor of around 150%, adding further evidence that it is the traffic source sector that contains the major error. There are several sources of disagreement between the flux emission estimates and those from the emission inventories. The emission inventories focus on longer term (annual) emission totals rather than providing estimates by hour of the year. For this reason the emissions for a particular hour of the year need to be estimated through the scaling factors described in the previous section. It is however difficult to quantify the additional uncertainties introduced when scaling factors are used in emission inventories in this way.

The London atmospheric emissions inventory

The London Atmospheric Emissions Inventory (LAEI) provides emission estimates for eight key air pollutants (including NO_x) at 1 km^2 resolution across all London boroughs, to the outer M25 motorway boundary that encompasses Greater London. The inventory reflects the geography of the roads in London, enabling an accurate assessment of population exposure and health impacts. The inventory is broken down into source sectors, contributing to the total annual estimates. Sources within the LAEI include: road transport (exhaust and non-exhaust), large regulated industrial processes, small regulated industrial processes, large boiler plants, gas heating (domestic and industrial-commercial), oil combustion sources (domestic and commercial), coal combustion sources (domestic and commercial), agricultural and natural sources, rail, ships, airports and others such as sewage plants. The LAEI also contains a non-road mobile machinery source (*e.g.* cranes, small electricity generators and other construction machinery), which has been shown previously to be a significant source of NO_x in central London.[13]

The LAEI uses a 'bottom up' road traffic inventory taking vehicle flow and speed on each road and combining these with national and London-specific vehicle stock data (including buses and taxis) to calculate emissions for each of the 11 vehicle types and combining these to create emissions at 1 km^2 resolution. The 'enhanced LAEI' results used here benefited from roadside emissions measurements, obtained using the University of Denver Fuel Efficiency Automobile Test (FEAT) system (IR/UV absorption spectroscopy), deployed for a 6 week campaign and taking measurements from 70 000 vehicles, including cars, buses and taxis, at four locations across London.[42] Vehicle number plates were recorded for each vehicle and these were cross-referenced against vehicle databases to obtain relevant vehicle details including their Euro emissions classification. The roadside emissions measurements quantified exhaust emissions of both total NO_x and NO_2 as a ratio to carbon dioxide (CO_2), with the results then combined with CO_2 estimates from the LAEI to create NO_x and NO_2 emissions in g km^{-1}. The emissions from vehicle types that were not measured during the campaign, most notably articulated heavy goods vehicles, were taken from the published LAEI results.[13]

In order to try to produce an improved agreement between the inventory measured emissions, we have produced an 'enhanced' version of the NAEI. We use all sources from the NAEI except its road emission source to form the base of the inventory. For the road emission source we use the enhanced LAEI road

emission estimates scaled using the described roadside emissions measurements data, which increases the road traffic source of NO_x in the inventory by an average of ∼50% across London. We also use a revised version of the LAEI's non-road mobile machinery (NRMM) source, which gives an improved estimate to that in the NAEI.

Comparing the enhanced NAEI with our measurements allows us to better assess the effect of using a more explicit treatment of traffic emissions in the national inventory. The same methodologies, as used for NAEI comparison, were used in analysis of the enhanced NAEI. Each enhanced NAEI source sector was analysed to give emission estimates along the flight track at 1 km resolution. Each sector was scaled individually to allow for time of day comparison using the scaling factors described earlier, then added together to give overall NO_x emission estimates.

Fig. 7 shows how enhanced NAEI emission estimates in red (standard error as light red shading) compare with the measured NO_x fluxes in blue (standard error as light blue shading) for each flight average. It is apparent that the agreement between the measurement and the inventory is better than for the standard NAEI. Outer regions of London seem to compare very well, with all flight legs showing only a small degree of discrepancy. However, despite the agreement being improved and almost always falling within the error of the 1 km spatially resolved flux measurement, there is still a significant discrepancy observed in central London. As with the standard NAEI data, the flight track was also divided into four parts, each approximately 11 km in length, with the flux data then averaged for each segment to give a single NO_x emission flux with reduced error (again in the range 30–45%). Fig. 8 depicts the average ratio of the measured to enhanced emission inventory flux from all the flight legs, with the error bars denoting the standard error of the 17 legs included, along with the source sector contribution as before. The contribution from the different source sectors is similar for the enhanced NAEI as for the standard inventory. The main difference is the addition of the non-road mobile machinery source, which now contributes up to 9% of total NO_x emissions in central London. The ratio of measurement to enhanced emissions inventory for all zones shows considerable improvement compared to the standard NAEI. For the SW outer London zones, the ratio is close to one (average of 1.1), which is within the standard error of the measurements. However, in central and NE London, there is still some significant underestimation (average measurement to inventory ratio of 1.48), which is outside the (30–
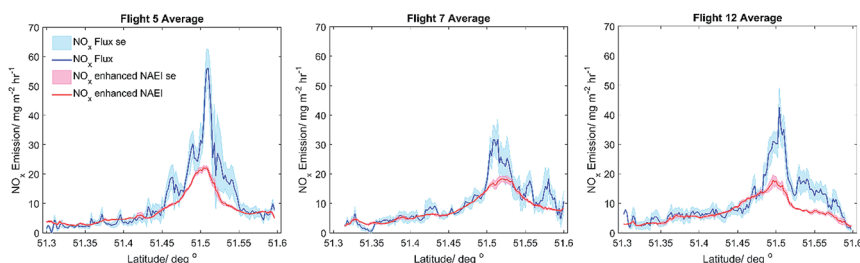

Fig. 7   Average for Flights 5, 7 and 12, measured NO_x flux plotted in blue with standard error as the shaded blue area. Calculated and scaled enhanced NAEI estimates of NO_x emission are plotted in red, with standard error as the shaded red area.
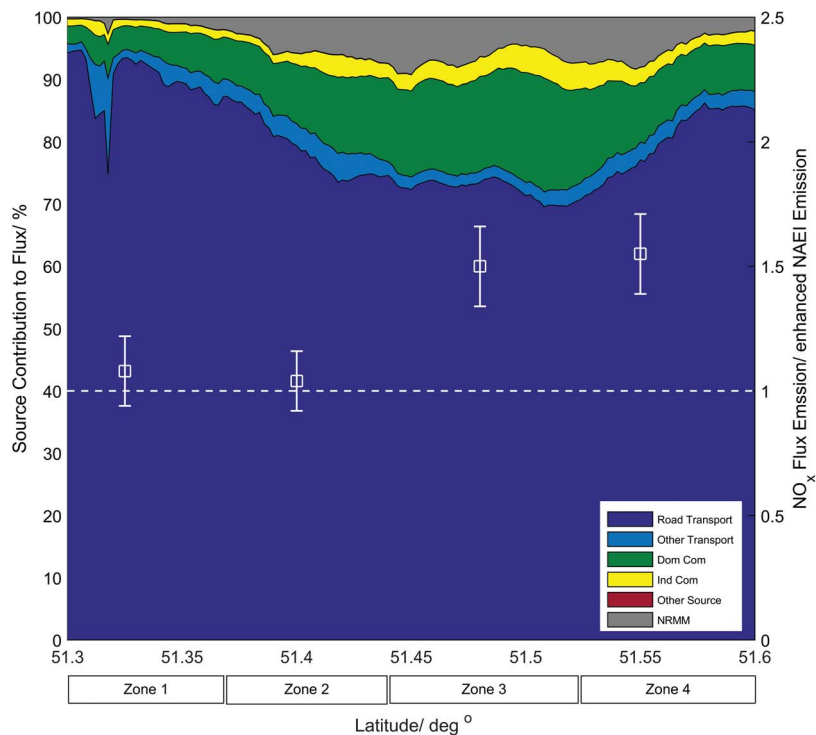
Fig. 8 Calculated emission source contributions from the enhanced NAEI (see text for details) plotted on the first y axis, with sources being broken down into road transport; other transport (such as rail), domestic combustion, industrial combustion, other sources and non-road mobile machinery (NRMM). Also plotted on the second y axis as white squares is the ratio of measured to enhanced NAEI estimated NO_x flux, with the error bars denoting the standard error of all points included. The flight is broken into 4 zones, with 1 and 2 being SW outer London, 3 central London and 4 NE outer London.

45%) flux measurement uncertainty. The observed improvements in the enhanced emission inventory estimation of NO_x can be directly related to the improved road transport source increasing the magnitude of the road transport emissions and the addition of the NMRR as a key source not currently accounted for in the standard NAEI.

Summary and conclusions

In this study, NO_x fluxes have been measured from an aircraft flying low over London using continuous wavelet transform, allowing for spatial analysis of NO_x emissions. NO_x fluxes were observed to be largest in central London, with maximum emissions of $\sim$80 mg m^{-2} h^{-1} observed on flights during the morning rush hour. After calculating flux footprints along the flight tracks, measurements were compared to scaled NAEI estimates, providing a top-down analysis of the inventory. A significant discrepancy was identified between NAEI emission estimates and actual flux measurements, with the highest underestimation being

a factor of two in central London. In outer London, where the source of NO_x is almost exclusively from road transport ($\sim$90%), there is an underestimation in the inventory of around a factor of 1.5, indicative of the poor treatment of the road traffic source in the NAEI. Due to the potential loss of some NO_x emitted at ground level during its transport to the measurement altitude, the calculated inventory underestimation can be considered as conservative.

We also compare our measurements to an enhanced version of the NAEI, containing both non-road mobile machinery emission sources from the LAEI and real world traffic emissions from the enhanced LAEI, which provides a much better treatment of NO_x coming from these sources. The comparison yielded better agreement between the two, especially in outer London, where the measured to inventory ratio was found to be around 1.1. In central London however there is still an average underestimation of around a factor of 1.5 compared to the measurements.

The current work has provided important information on the spatial variation in NO_x emissions over a large and complex urban environment. There are several areas where further research would be beneficial. First, the inhomogeneous terrain in London presents a challenge for flux measurements, both in terms of the inhomogeneous nature of the roughness and distributions of emissions (horizontally and vertically). Further measurements over different city areas would help better understand these effects. For example, measurements over a city such as Paris that has fewer high-rise buildings than London would provide a useful contrast. Second, the measurement of the fluxes of other species such as CO and CO_2 would help provide more comprehensive analysis of the NO_x flux emission estimates. More work is also required on understanding and quantifying the short-term accuracy of emission inventories. Emission inventories tend to focus on providing longer term (annual) emission estimates and are less able to provide information on the temporal nature of emissions. Improved information on the temporal characteristics of emissions would improve the reliability of short-term flux measurements when compared with emission inventories. In particular, our measurements highlight the critical importance of obtaining independent measurements of pollutant emission rates from vehicles during on-road driving conditions and using these data in emission inventories, rather than relying on emissions data obtained during artificial test driving conditions or provided by vehicle manufacturers.

Author contribution statement

CNH, ACL, JL and RP conceived the study and obtained funding. AV and JL wrote the paper. AV, SM, PM, AG and TK carried out the flux data analysis and footprint modelling. JL, MS, ACL, CNH, RP and BD made the measurements. DC and SB provided the emissions inventory and scaling data, as well as help in interpreting the results. All authors contributed to the discussion and commented on the manuscript.

Acknowledgements

References

1 V. Strand, M. Svartengren, S. Rak, C. Barck and G. Bylin, *Eur. Respir. J.*, 1998, **12**, 6–12.

2 R. W. Atkinson, I. M. Carey, A. J. Kent, T. P. van Staa, H. R. Anderson and D. G. Cook, *Epidemiology*, 2013, **24**, 44–53.

3 WHO, *Review of evidence on health aspects of air pollution – REVIHAAP project: final technical report*, 2013.

4 WHO, *Health risks of air pollution in Europe – HRAPIE project, Recommendations for concentration–response functions for cost–benefit analysis of particulate matter, ozone and nitrogen dioxide*, 2014.

5 S. Sillman, *Atmos. Environ.*, 1999, **33**, 1821–1845.

6 D. C. Carslaw, S. D. Beevers, J. E. Tate, E. J. Westmoreland and M. L. Williams, *Atmos. Environ.*, 2011, **45**, 7053–7063.

7 D. C. Carslaw, *Atmos. Environ.*, 2005, **39**, 4793–4802.

8 M. Weiss, P. Bonnel, R. Hummel, A. Provenza and U. Manfredi, *Environ. Sci. Technol.*, 2011, **45**, 8575–8581.

9 E. A. Mazzi and H. Dowlatabadi, *Environ. Sci. Technol.*, 2007, **41**, 387–392.

10 T. Bush, I. Tsagatakis, K. King and N. Passant, *NAEI UK emission mapping methodology 2006*, 2008.

11 J. Brioude, S. W. Kim, W. M. Angevine, G. J. Frost, S. H. Lee, S. A. McKeen, M. Trainer, F. C. Fehsenfeld, J. S. Holloway, T. B. Ryerson, E. J. Williams, G. Petron and J. D. Fast, *J. Geophys. Res.: Atmos.*, 2011, **116**, 19.

12 J. D. Lee, C. Helfter, R. M. Purvis, S. D. Beevers, D. C. Carslaw, A. C. Lewis, S. J. Moller, A. Tremper, A. Vaughan and E. G. Nemitz, *Environ. Sci. Technol.*, 2015, **49**, 1025–1034.

13 Greater London Authority, London Datastore, http://data.london.gov.uk/.

14 M. D. Shaw, J. D. Lee, B. Davison, A. Vaughan, R. M. Purvis, A. Harvey, A. C. Lewis and C. N. Hewitt, *Atmos. Chem. Phys.*, 2015, **15**, 5083–5097.

15 J. D. Lee, S. J. Moller, K. A. Read, A. C. Lewis, L. Mendes and L. J. Carpenter, *J. Geophys. Res.: Atmos.*, 2009, **114**, DOI: 10.1029/2009jd011879.

16 I. B. Pollack, B. M. Lerner and T. B. Ryerson, *J. Atmos. Chem.*, 2010, **65**, 111–125.

17 K. M. Beswick, M. W. Gallagher, A. R. Webb, E. G. Norton and F. Perry, *Atmos. Chem. Phys.*, 2008, **8**, 5449–5463.

18 C. Torrence and G. P. Compo, *Bull. Am. Meteorol. Soc.*, 1998, **79**, 61–78.

19 C. Thomas and T. Foken, *Boundary-Layer Meteorology*, 2007, **123**, 317–337.

20 B. Yuan, L. Kaser, T. Karl, M. Graus, J. Peischl, T. L. Campos, S. Shertz, E. C. Apel, R. S. Hornbrook, A. Hills, J. B. Gilman, B. M. Lerner, C. Warneke,

F. M. Flocke, T. B. Ryerson, A. B. Guenther and J. A. de Gouw, *J. Geophys. Res.: Atmos.*, 2015, **120**, 6271–6289.

21 S. Metzger, W. Junkermann, M. Mauder, K. Butterbach-Bahl, B. T. Y. Widemann, F. Neidl, K. Schafer, S. Wieneke, X. H. Zheng, H. P. Schmid and T. Foken, *Biogeosciences*, 2013, **10**, 2193–2217.

22 A. Held, *Boundary-Layer Meteorology*, 2014, **151**, 79–94.

23 T. Karl, E. Apel, A. Hodzic, D. D. Riemer, D. R. Blake and C. Wiedinmyer, *Atmos. Chem. Phys.*, 2009, **9**, 271–285.

24 T. Karl, P. K. Misztal, H. H. Jonsson, S. Shertz, A. H. Goldstein and A. B. Guenther, *J. Atmos. Sci.*, 2013, **70**, 3277–3287.

25 P. K. Misztal, T. Karl, R. Weber, H. H. Jonsson, A. B. Guenther and A. H. Goldstein, *Atmos. Chem. Phys.*, 2014, **14**, 10631–10647.

26 R. Atkinson, *Atmos. Environ.*, 2000, **34**, 2063–2101.

27 J. Mann and D. H. Lenschow, *J. Geophys. Res.: Atmos.*, 1994, **99**, 14519–14526.

28 H. P. Schmid, *Agr. Forest Meteorol.*, 2002, **113**, 159–183.

29 T. Vesala, U. Rannik, M. Leclerc, T. Foken and K. Sabelfeld, *Agr. Forest Meteorol.*, 2004, **127**, 111–116.

30 T. Vesala, N. Kljun, U. Rannik, J. Rinne, A. Sogachev, T. Markkanen, K. Sabelfeld, T. Foken and M. Y. Leclerc, *Environ. Pollut.*, 2008, **152**, 653–666.

31 M. Y. Leclerc and T. Foken, *Footprints in micrometeorology and ecology*, Springer, 2014.

32 S. Metzger, W. Junkermann, M. Mauder, F. Beyrich, K. Butterbach-Bahl, H. P. Schmid and T. Foken, *Atmos. Meas. Tech.*, 2012, **5**, 1699–1717.

33 D. R. Drew, J. F. Barlow and S. E. Lane, *J. Wind Eng. Ind. Aerod.*, 2013, **121**, 98–105.

34 D. C. Carslaw and S. D. Beevers, *Atmos. Environ.*, 2004, **38**, 3585–3594.

35 Defra and DECC, NAEI data, http://naei.defra.gov.uk/.

36 EEA, *EMEP/EEA air pollutant emission inventory guidebook 2013, Technical guidance to prepare national emission inventories*, Report 12/2013, 2013.

37 D. P. Billesbach, *Agr. Forest Meteorol.*, 2011, **151**, 394–405.

38 J. D. Lee, L. K. Whalley, D. E. Heard, D. Stone, R. E. Dunmore, J. F. Hamilton, D. E. Young, J. D. Allan, S. Laufs and J. Kleffmann, *Atmos. Chem. Phys. Discuss.*, 2015, **15**, 22097–22139.

39 A. Bjorkegren, C. Grimmond, S. Kotthaus and B. Malamud, *Atmos. Environ.*, 2015, **122**, 775–790.

40 A. R. Desai, K. Xu, H. Tian, P. Weishampel, J. Thom, D. Baumann, A. E. Andrews, B. D. Cook, J. Y. King and R. Kolka, *Agr. Forest Meteorol.*, 2015, **201**, 61–75.

41 D. H. Lenschow, D. Gurarie and E. G. Patton, *Geoscientific Model Development Discussions*, 2015, **8**, 9323–9372.

42 D. C. Carslaw and G. Rhys-Tyler, *Atmos. Environ.*, 2013, **81**, 339–347.